Ferroelectrics, 1999, Vol. 226, pp. 243–261
Reprints available directly from the publisher
Photocopying permitted by license only

DIPOLE ORDERING AND CRITICAL BEHAVIOR OF THE STATIC AND DYNAMIC PROPERTIES IN THREE-DIMENSIONAL AND LAYERED $MM'P_2X_6$ CRYSTALS (M, M' – Sn, Cu, In; X – S, Se)

YU. M. VYSOCHANSKII[a,*], A. A. MOLNAR[a], V. A. STEPHANOVICH[a], V. B. CAJIPE[b] and X. BOURDON[b]

[a] *Institute for Solid State Physics and Chemistry, Uzhgorod University, Uzhgorod, 294000, Ukraine;*
[b] *Institut des Materiaux de Nantes, B.P. 32229, 44322, Nantes, Cedex 3, France*

(Received in final form 17 July 1998)

The thermodynamic properties and lattice dynamics of crystals $MM'P_2X_6$ with cations in different valence states have been investigated. For $Sn_2P_2S(Se)_6$ crystals with a three-dimensional lattice, the interaction between polarization and deformation plays an important role in the mechanisms of the displacive transitions from a paraelectric to ferroelectric or incommensurate phase in the vicinity of a Lifshitz point on the state diagram. Layered $CuInP_2S_6$ crystals undergo a first order and order–disorder type phase transition to a ferrielectric phase. For these crystals, different polarization mechanisms within a wide frequency range were clearly observed and found to be interrelated *via* dielectric and Raman spectroscopy measurements. These mechanisms include the internal vibrations of $(P_2S_6)^{4-}$ anions; the external lattice modes in which In^{3+} and Cu^+ ions participate; the relaxational critical slowing-down due to Cu^+ ions which yield the order–disorder phase transition; and the low frequency relaxational dynamics which causes the "throw" of Cu^+ ions into the interlayer space thus providing ionic conductivity.

Keywords: Phase transitions; ferroelectrics; ferrielectrics; dielectric properties; Raman scattering; lattice dynamics

* Corresponding author.

INTRODUCTION

Recent years have seen the emergence of relatively new ferroelectric materials belonging to the chalcogenophosphate family.[1-3] These compounds contain $(P_2X_6)^{4-}$ anions (X = S or Se) which are linked together by the cations. Because the ethane-like groups are able to withstand variations in P—P and P—X bond lengths, a large number of chalcogenophosphates have been prepared.[4] Moreover, the coordination preferences of different cations have led to two types of morphologies, *i.e.*, either a three-dimensional or lamellar structure. The nature of dipole ordering derives from bonding, Coulomb and elastic effects peculiar to a given lattice and may thus be expected to be different in each class.

The first category is typified by $Sn_2P_2S_6$ in which the tin ions are formally in the divalent oxidation state. The Sn^{2+} polyhedra have an average coordination of eight thus yielding a three-dimensional connectivity for the $(P_2S_6)^{4-}$ anions. $Sn_2P_2S_6$ undergoes a second-order ferroelectric-paraelectric transition around 337 K while $Sn_2P_2Se_6$ exhibits an incommensurate and ferroelectric phase below 221 and 193 K, respectively.[1,2] It is conceivable that a localization of the lone pair of electrons for divalent tin plays a role in the appearance of ferroelectricity in these materials. However, Pb^{2+} which likewise has a lone pair has not been observed to move off-center in isostructural crystals of $Pb_2P_2S_6$ even at temperatures close to 0K.[5] Both tin and lead can assume a 4+ oxidation state but only tin has been found to form another thiophosphate, lamellar SnP_2S_6[6] (see below), in which it is embedded in an octahedral environment. This possibility of a six or eight chalcogen coordination for tin probably promotes the transitions in $Sn_2P_2S(Se)_6$.[2,7] It is worth mentioning that the SnP_2S_6 structure has been shown to feature slightly off-center Sn^{4+} ions but no phase transition has yet been detected therein.

The second category is best represented by $CuMP_2S_6$ (M = Cr or In) in which copper is formally monovalent and M is trivalent.[3,8,9] These compounds consist of lamellae defined by a sulfur framework which provides octahedral voids for the metal cations and P—P pairs. Within a layer, the Cu, M and P—P pairs. Within a layer, the Cu, M and P—P form triangular patterns. Dipole ordering in these materials requires antiparallel displacements of the d^{10} cations: whereas the copper sublattice is antipolar in $CuCrP_2S_6$ at $T < 150$ K,[8] it is polar in $CuInP_2S_6$ below $T_c \sim 315$ K and coexists with an In^{3+} sublattice of unequal and opposite polarity. The cation off-centering is attributable to a second-order Jahn-Teller instability associated with the d^{10} electronic configuration; the

lamellar matrix absorbs the structural deformations *via* the flexible $(P_2S_6)^{4-}$ groups.[3,9] Interestingly enough, Sn^{4+} is a d^{10} cation so that off-centering in SnP_2S_6 might also be ascribed to a pseudo Jahn-Teller effect.

The phase transition (PT) in $Sn_2P_2S_6$ type crystals is second-order, displacive and has been extensively studied both experimentally and theoretically the past two decades. The mechanism for the PT may be described in terms of an interaction between the branches of the soft optical mode and acoustic modes.[10] Within the phase diagram of $Sn_2P_2(Se_xS_{1-x})_6$ solid solutions, this interaction determines the presence of a Lifshitz point at $x \sim 0.28$ and the appearance of an incommensurate phase at $x > 0.28$.[2] The connection between the spontaneous polarization and the elastic deformations also determines the temperature dependences of the thermodynamic properties across the incommensurate phase, especially near the lock-in transition.[11] The anisotropy of a given system defines the peculiar critical anomalies of properties near the Lifshitz point of a system with strong uniaxial dipolar interaction which represents a new universality class.[12] A renormalized-group analysis[12] predicts mean-field critical behavior of the thermodynamic functions with specific multiplicative corrections. Such behavior was observed in the investigation of the dielectric properties of $Sn_2P_2S_6$ crystals.[13] Further enriching this variety of phenomena is the semiconducting character of these compounds. It has been found that the temperature width of the incommensurate phase and the coordinates of Lifshitz point depend on the degree of non-equilibrium of the electron subsystem in these semiconducting ferroelectrics.[13]

Some aspects of the phase transitions in the lamellar thiophosphates have been investigated. The paraelectric phase of $CuMP_2S_6$ (M = Cr or In) can be described in the monoclinic space group C2/c and is characterized by a distribution of the Cu^+ over sites within an octahedral S_6 cage and disposed along the normal to the layers. The PT in these systems is triggered by the appearance of an ordered copper sublattice and is thus of the order–disorder type. In $CuCrP_2S_6$, the Cu^+ ions freeze into an quasi-antipolar state between 191 and 175 K, and then form an antiferroelectric array of dipoles below 150 K (space group Pc).[8] At $T < 315(5)$ K, symmetry lowering in $CuInP_2S_6$ results not only from copper ordering but also the off-centering of In^{3+} ions (space group Cc). Earlier calorimetry and dielectric measurements indicate that this PT is first order.[3] The spontaneous polarization P_s appears along the normal to the layer as a result of the ferrielectric contributions P_s(Cu) and P_s(In). Aside from this, Cu^+ ions are

known to be present in the interlayer space at $T > T_c$, [9] *i.e.*, ionic conduvtivity occurs. [14]

There had been some controversy about the nature of the copper disorder (static or dynamic) in the non-polar phase of $CuMP_2S_6$. [15] In addition, it is possible that the PT in $CuInP_2S_6$ involves a displacive component due to the In^{3+} off-centering. More generally, $CuMP_2S_6$ may be considered as an unusual model system for the study of cooperative dipole effects in a two-dimensional matrix. It would thus be of interest to investigate the critical behavior of static and dynamic properties in these layered thiophosphates. Also, one may expect new peculiarities to accompany dipole ordering in compounds which exhibit ionic conductivity. Within this context, we have performed dielectric and Raman spectroscopy measurements on crystals of $CuInP_2S_6$. We present these results in this work.

EXPERIMENTAL METHODS

Crystals of $CuInP_2S_6$ were prepared as previously described. [3] The specimens were about $4 \times 3 \times 0.2$ mm^3 in size. Silver paste was applied to the (001) faces for electrical contacts, *i.e.*, dielectric measurements were made perpendicular to the crystal layers. The temperature dependence of the electric permittivity was measured using computer controlled equipment. [13] Accuracies were 0.1% for the real part ε' and 0.5% for the imaginary part ε'' of the complex permittivity. A 50 mV electric field was applied and measurements were performed in the $10-10^5$ Hz frequency range under dark conditions. The sample was annealed for one hour before measurement; temperature changes were made at a rate of 0.1 K/min.

For the Raman scattering investigation the orthogonal $X(ZZ)Y$ light scattering geometry was used. The X and Y Cartesian axes coincide with a and b in the plane of the layer while the Z axis coincides with the direction normal to the layers (c^*). Polarized radiation from a He–Ne gas laser with wavelength 6328 Å and power near 30 mW provided the excitation. The radiation was focused on the face of a layered crystal. The right angle scattering exited across the face of the investigated crystal and was analyzed by a DFS-24 two-grating spectrometer with a spectral resolution near 2 cm^{-1}. The specimens were loaded under nitrogen vapor in a UTRECS cryostat. The sample temperature was controlled with 0.5 K accuracy. The susceptibility was determined from the Raman scattering spectra. The spectra were analyzed *via* a decomposition into Lorentz lines.

DIELECTRIC MEASUREMENTS

The anomalies in the thermal variation of the real ε' and imaginary ε'' parts of the electric permittivity of $CuInP_2S_6$ crystal near the PT appear most clearly with a measurement frequency of 10^5 Hz (Fig. 1). In the paraelectric phase, Curie-Weiss behavior $\varepsilon' = C(T - T_0^+)^{-1}$ is observed and found to be consistent with a constant $C = 4700$ and a Curie-Weiss temperature $T_0 \sim 300$ K ($\varepsilon'^{-1}(T) \to 0$ as $T \to T_0^+$). At the first-order paraelectric–ferrielectric transition the value of ε' drops appreciably. The transition temperature is deduced from the T value corresponding to the maximum derivative of ε' which is $T_c \sim 323$ K. A step change at the transition is also evident in the curve for ε'' which is proportional to the dielectric loss. It is worth nothing that the value of ε'' is large in the entire temperature range investigated within the paraelectric regime.

ε' and ε'' were measured at various frequencies during both heating and cooling runs (Figs. 2, 3). Thermal hysteresis for the anomalies close to the PT is clearly observed, having a width of about 3K. Such a hysteresis expected of a first-order phase transition.

Decreasing the measuring field frequency causes a rise in ε' at T_c (Fig. 2) and pronounced deviation from the Curie-Weiss law for ε'^{-1} (T) in the paraelectric phase.

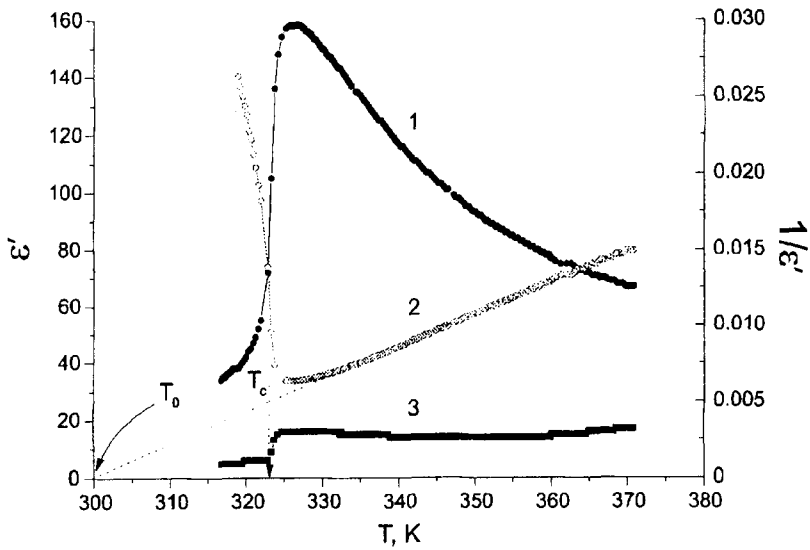

FIGURE 1 Temperature dependence in cooling mode of $CuInP_2S_6$ crystal dielectric parameters at a 10^5 Hz frequency: $1 - \varepsilon'$; $2 - 1/\varepsilon'$; $3 - \varepsilon''$.

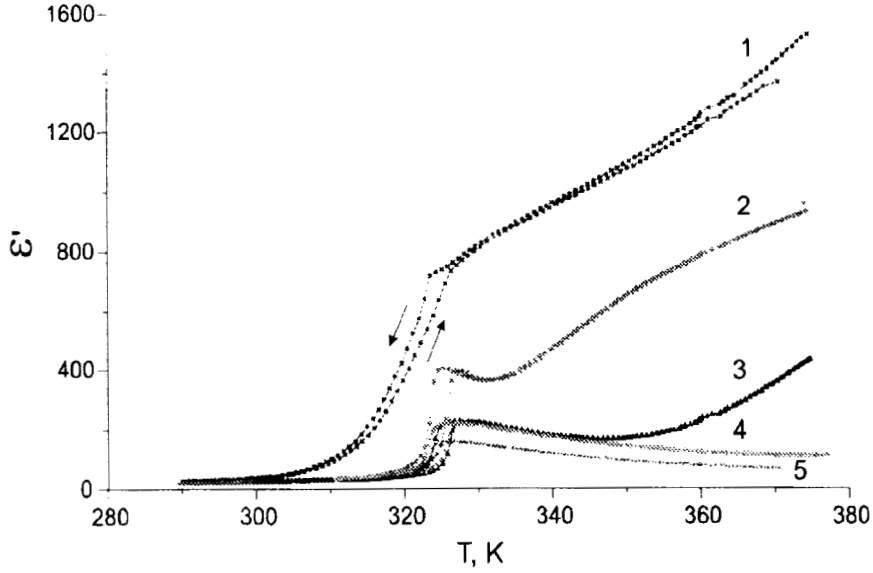

FIGURE 2 The temperature dependence of the real part of the electric permittivity ε' upon cooling and heating at different frequencies: 1 – 10; 2 – 10^2; 3 – 10^3; 4 – 10^4; 5 – 10^5 Hz.

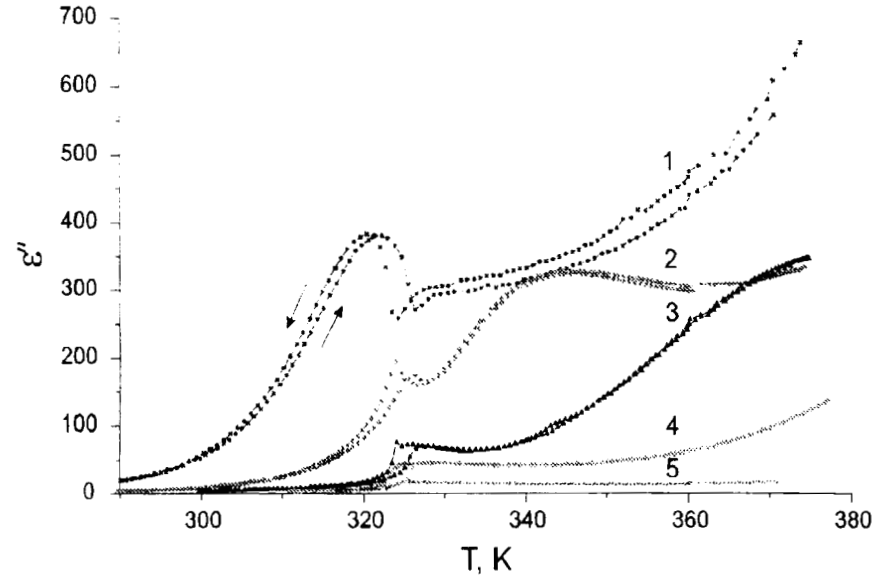

FIGURE 3 The temperature dependence of the imaginary part of the electric permittivity ε'' upon cooling and heating at different frequencies: 1 – 10; 2 – 10^2; 3 – 10^3; 4 – 10^4; 5 – 10^5 Hz.

The latter is indicative of low frequency polarization mechanisms. The existence of these mechanisms is evident in their contribution to $\varepsilon''(T)$ measured at different frequencies (Fig. 3). Two low frequency mechanisms of polarization may be assumed in addition to those originating from the critical slowing down of the PT order parameter fluctuations. These may be related to the following features. First, a maximum is observed in the $\varepsilon''(T)$ curve at a temperature which decreases as the measuring field frequency is reduced. Second, at the lowest 10 and 100 Hz frequencies, ε'' rises with increasing temperature in the paraelectric phase. These low frequency curves also exhibit additional dielectric contribution at $T < T_c$ (Figs. 2, 3).

The Cole–Cole diagrams clearly demonstrate the existence of two low frequency mechanisms of polarization (Fig. 4). The lowest frequency dispersion is most probably ascribable to ionic conductivity: its contribution

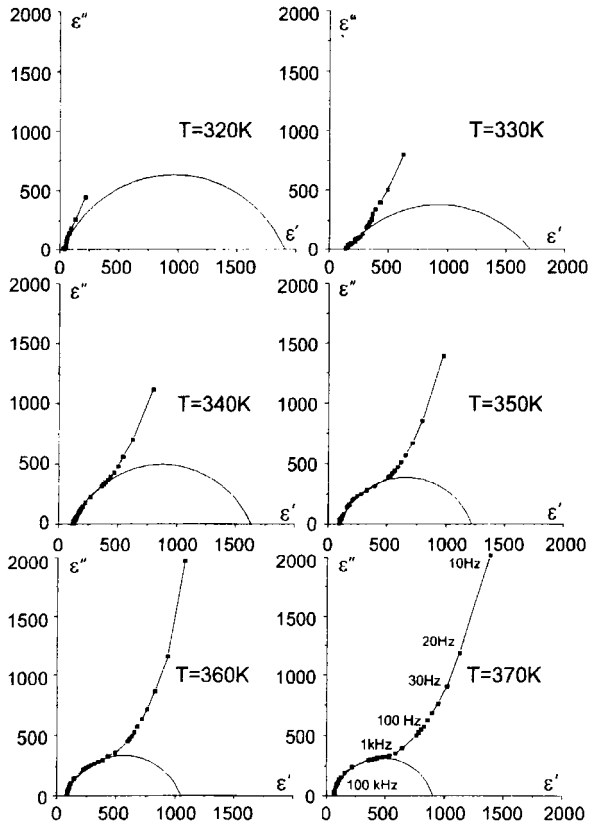

FIGURE 4 Cole–Cole diagrams for $CuInP_2S_6$ at various temperatures.

vanishes at $T < 300$ K and increases with crystal heating in the paraelectric phase. More quantitatively, the relaxational polarization effects may be extracted *via* the Debye equation which describes them

$$\varepsilon^* = \varepsilon' - i \cdot \varepsilon'' = \varepsilon_\infty + \frac{\varepsilon_0 - \varepsilon_\infty}{(1 + \omega^2 \cdot \tau^2)} - i \cdot \frac{(\varepsilon_0 - \varepsilon_\infty) \cdot \omega \cdot \tau}{1 + \omega^2 \cdot \tau^2}, \qquad (1)$$

where: τ is the relaxation time for a given polarization mechanism; $\varepsilon' = \varepsilon_0$ at $\omega = 0$; and, $\varepsilon'' = \varepsilon_\infty$ at $\omega \gg \tau^{-1}$

The equation of a circle follows from the coordinates ε'' and ε' in Eq. (1). Circular arcs are extrapolated from the curve defined by the high frequency data. Spectral "smearing", *i.e.*, the existence of distribution of relaxation times, causes the center of these semicircles to shift away from the ε' axis.

The smearing is greatest in the vicinity of T_c as shown by the data for 330 K. The temperature dependence of ε_∞ determined from the complex permittivity diagrams coincides with that of ε' (T) measured at 10^5 Hz (Fig. 5). The value of ε_0 decreases as the temperature rises, in agreement with the temperature behavior of a polarizibility due to a thermal polarization mechanism.

The data show that the relaxation frequency increases with crystal heating in the paraelectric phases. For relaxation dynamics, the temperature

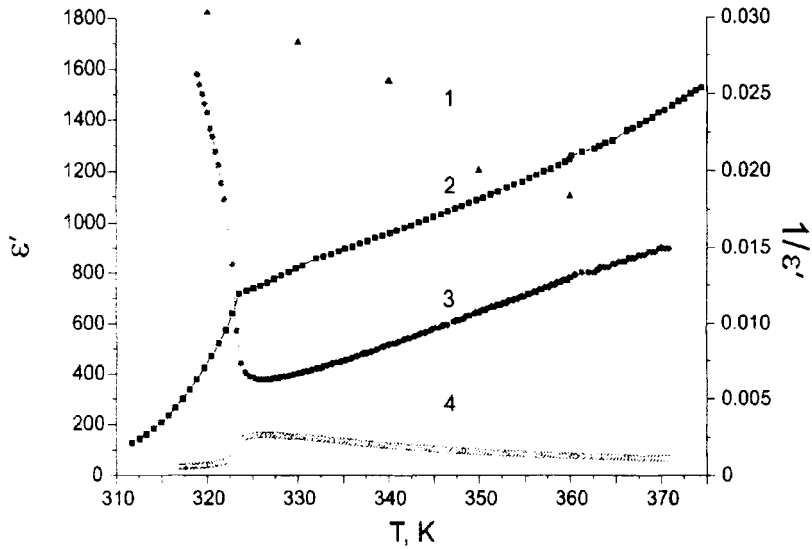

FIGURE 5 Comparison of the temperature dependence in cooling mode of ε_0 – 1; ε' at 10 Hz – 2, $1/\varepsilon'$ at 10^5 Hz – 3; and ε' at 10^5 Hz – 4.

behavior of the relaxation time usually satisfies an Arrhenius law

$$\tau = \tau_0 \cdot e^{\frac{U}{kT}}. \tag{2}$$

In such a case, plotting In τ^{-1} *versus* T^{-1} yields an activation energy $U \sim 1.17$ eV.

In summary, the dielectric measurement data for $CuInP_2S_6$ allow us to conclude that three mechanisms of polarization exist in the investigated temperature range.

The high frequency polarization mechanism is related to the first-order, order–disorder type PT. Its dielectric contribution (ε_∞ in our notation) measured at 10^5 Hz sastifies a Curie-Weiss law $\varepsilon' = C(T - T_0)^{-1}$ with $T_0 \sim 300$ K and $C \sim 4700$ K. The structural PT order parameter fluctuations evidently contain two components. One of them is relaxational in nature and due to copper hopping motions within a double-well potential defined by the S_6 cage and which are directed along the normal to the layer. The other is oscillatory and attributable to the In atom shifting away from a centrosymmetric site. The first component was recently observed in neutron spectra *via* 5–10–cm^{-1}-wide quasielastic scattering while the second manifested as a softening phonon in light scattering experiments (see below).

A low frequency mechanism of relaxational polarization appears at frequencies below 10^3 Hz. Its spectrum satisfies the Debye dispersion relation. At $T > T_c$ the temperature dependence of the relaxation frequency satisfies the Arrhenius law which describes the thermal polarization in the simplest approximation; an activation energy $U \sim 1.17$ eV is found. The dielectric contribution $\varepsilon_0 - \varepsilon_\infty$ of this polarization mechanism increases with cooling (Fig. 5). From Eqs. (1) and (2) the value of ε' at fixed frequency, for example at 10 Hz, decreases with decreasing temperature in the paraelectric phase. Also it is important to note the break in the 10 Hz $\varepsilon'(T)$ curve. The temperature at which this break occurs coincides with that of the jump in the $\varepsilon'^{-1}(T)$ curve measured at 10^5 Hz. This fact confirms the necessity of taking into account the renormalization of the activation energy by the spontaneous polarization at $T < T_c$. In the simplest approach, $U_F = U_P + aP_s^2$. The sudden increase of the activation energy at the PT into the acentric phase slows down the relaxation process of the repolarization of the sample in the measured field. Consequently, the dielectric contribution from this polarization mechanism disappears even at a very low frequency of 10 Hz. At $T < 300$ K this component of the thermal polarization practically "freezes". The low frequency dielectric contribution is probably defined by the thermal "throw" of Cu atoms into the interlayer

van-der-Waals gap. This is consistent with crystallographic evidence for a non-zero probability of finding Cu atoms in the interlayer space at $T > 300$ K which is enhanced by heating. [9]

The "tail" in the Cole–Cole diagrams (Fig. 4) points to the presence of dielectric contributions which increase as $\omega \to 0$. This means that conductivity is present in the sample. As seen in curves 1 and 2 of Figure 5, the conductivity causes an overlap at high temperatures ($T > 350$ K) between the temperature variation of ε' measured at 10 Hz and that of the dielectric contribution ε_0 calculated for the previous relaxational polarization mechanism. In $CuInP_2S_6$, the conductivity by Cu^+ ionic transport obviously dominates. Such ionic conductivity has indeed been observed in $CuInP_2S_6$ [14] as well as in isomorphic $(Mn_{0.78}Cu_{0.26})P_2S_6$ crystals. [6] From the complex permittivity diagrams (Fig. 4) the temperature dependence of the dielctric loss related with conductivity may be determined. Assuming that such ionic transport has activation character, an estimate for the activation energy may be obtained by plotting $\ln \Delta\varepsilon = f(T^{-1})$ which yields $U_{tr} \sim 0.5$ eV, a value consistent with that found in an earlier study. [14]

The three mechanisms of polarization in $CuInP_2S_6$ are interrelated. The disappearance of spontaneous polarization with crystal heating leads to an increased probability of Cu^+ ions being "thrown" into van-der-Waals gaps. Such thermal "throws" are a prerequisite to the appearance of ionic conductivity.

RAMAN SCATTERING MEASUREMENTS

The Raman spectrum of $CuInP_2S_6$ recorded around 100 K in the $X(ZZ)Y$ scattering geometry displays twenty bands. [17] As the temperature increases, the most pronounced changes occur at frequencies less than 350 cm^{-1}: the spectral lines change their width, shape and relative intensities (Fig. 6). In the paraelectric phase, the number of observed lines is two times smaller while the linewidth of the bands increases almost threefold.

For the line close to 250 cm^{-1} in the 95 K spectrum, the width increases to 9 cm^{-1} upon heating to 300 K and then rapidly rises to 13 cm^{-1} at 320 K (Figs. 7, 8). It is remarkable that this width does not increases above 320 K. Such T-dependence of is consistent with the occurrence of first-order PT in $CuInP_2S_6$ at $T_c \sim 323$ K. Similar behavior is observed in the temperature dependence of the peak intensities of the bands near 240 and 268 at 95 K (Fig. 8). The largest rate pf temperature change of these peak intensities is also observed in the 300–323 K interval.

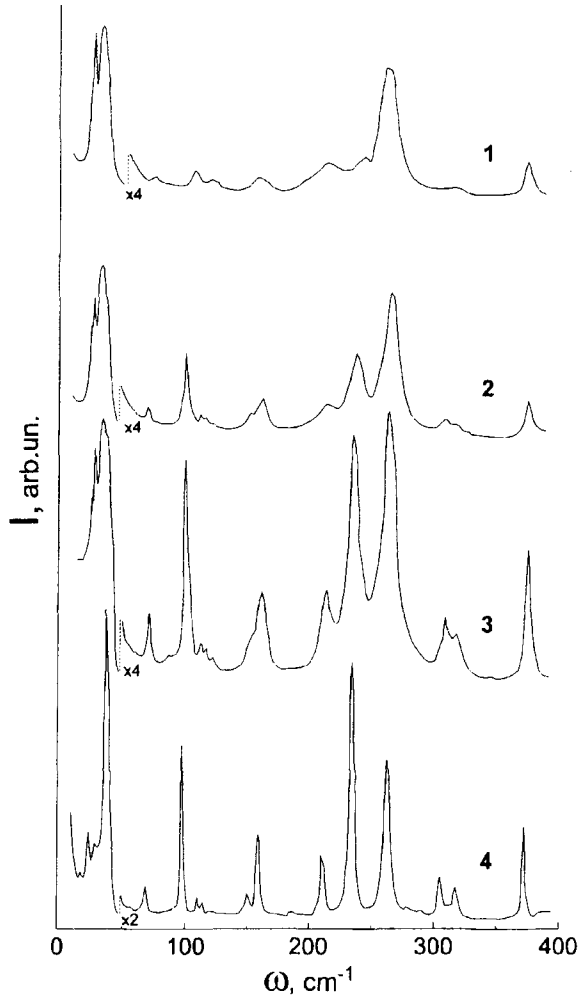

FIGURE 6 The Raman scattering spectra of $CuInP_2S_6$ crystal in $X(ZZ)Y$ geometry at different temperatures: 1 – 340 K, 2 – 300 K, 3 – 250 K, 4 – 120 K.

A complex transformation of the Raman spectrum is observed in the low energy range ($< 60\,cm^{-1}$) and may be related to the PT (Fig. 9). Three bands – near 28, 33 and $42\,cm^{-1}$ – are clearly observed at 95 K. A weak band close to $22\,cm^{-1}$ also appears at higher temperatures. The highest energy band of this group moves from 42 to $34\,cm^{-1}$ as the temperature is raised to 300 K, *i.e.*, still within the ferroelectric phase. Simultaneously, a marked intensity redistribution among the low-energy bands intensities occurs. The

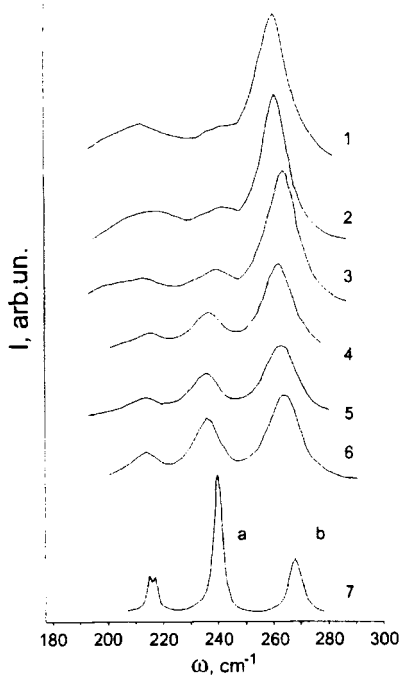

FIGURE 7 The temperature dependence of the spectral lines of the internal deformational modes of $(P_2S_6)^{4-}$ ions in $CuInP_2S_6$ crystals. 1 – 370 K, 2 – 329 K, 3 – 319 K, 4 – 311 K, 5 – 306 K, 6 – 299 K, 7 – 95 K.

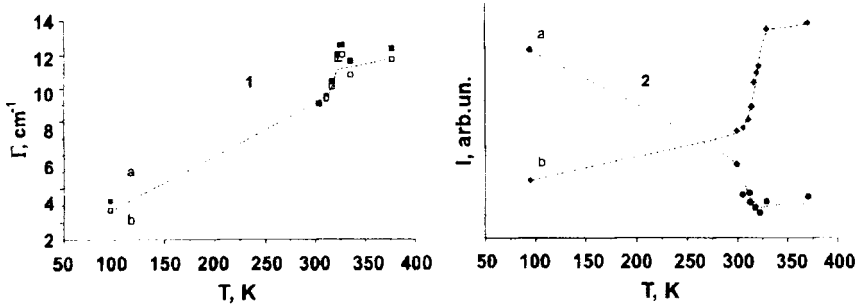

FIGURE 8 The temperature dependence of the damping (1) and the peak intensity (2) of the spectral lines from Figure 7.

biggest variation of the low frequency spectrum is observed in the 300 – 323 K interval (Fig. 10).

The symmetry analysis of the lattice vibrations in $CuInP_2S_6$ crystals and the identification of the Raman spectral lines based on known phonon

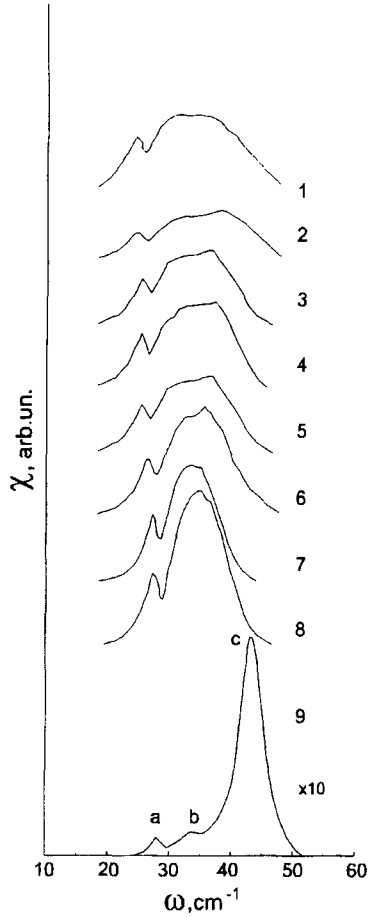

FIGURE 9 The temperature evolution of the susceptibility, which was determined from the Raman spectra of the $CuInP_2S_6$ crystal in the region of the external vibration of the lattice 1–370 K, 2–329 K, 3–312 K, 4–319 K, 5–316 K, 6–311 K, 7–306 K, 8–299 K, 9–95 K.

spectra for crystals within the $M^{4+}P_2X_6 - M_2^{2+}P_2X_6 - M^+M^{3+}P_2X_6$ series [17] would serve as a background for understanding the temperature variations mentioned above.

The structure of $CuInP_2S_6$ in the paraelectric phase is described in the C2/c (2/m or C_{2h}) space group with four formula units in the elementary cell. [3, 18] The primitive cell, which determines the number of the normal vibrations at the center of the Brillouin zone, contains two formula units within a single layer. Structural results [9, 18] give the following site symmetries for the atoms: C_2 for Cu and In in two-fold symmetric sites, and C_1 for P and S in a general crystallographic positions. Symmetry

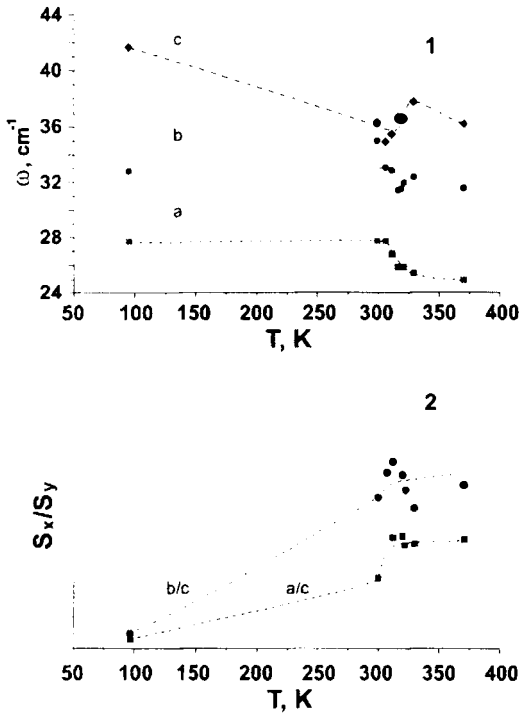

FIGURE 10 The temperature dependence of the low energy spectral line frequencies (1) and their relative integrated intensities (2).

analysis then yields the modes as

$$\Gamma_{opt} = 14A_g + 16B_g + 13A_u + 14B_u, \text{ and } \Gamma_{acoust} = A_u + 2B_u.$$

In the ferrielectric phase (space group Cc, point group *m* or Cs) the primitive cell also contains two formula units. The expected vibrational modes are

$$\Gamma_{opt} = 28A' + 29A'', \text{ and } \Gamma_{acoust} = 2A' + A''.$$

The symmetry analysis for the paraelectric and ferrielectric phase follows from correlating the irreducible representation of the symmetry group D_{3d} of the $(P_2S_6)^{4-}$ anions- and those of the atomic positions (C_1 or C_2) with the factor-group (2/m or m) of the crystal.

The $(P_2S_6)^{4-}$ anions are in general positions of the $CuInP_2S_6$ sturcture. For this reason 18A internal anionic modes occur. These split into 36A modes *via* a resonant interaction between two anions in a primitive cell. The external translation and libration modes yield 12A vibrations. In the

paraelectric phase the translations of the metal atoms in C_2 positions have the irreducible representation $\Gamma = 4A + 8B$. Here, the translations along the crystallographic b axis are fully symmetric.

We may now identify the bands in Raman spectrum of $CuInP_2S_6$ crystals. First we will determine the frequency range of the internal vibrations of the $(P_2S_6)^{4-}$ anion. From the Raman spectra analysis for $Sn(Pb)_2P_2S_6$ crystals [19] it was found that the internal vibrations have frequencies in the interval $160-600\,cm^{-1}$. We can extract four characteristic groups of internal vibrations. These groups we will refer to as $\nu P—S$, $\nu P—P$, $\nu S—P—S$ and $\nu S—P—P$. The valence vibrations $\nu P—S$ of the PS_3 groups, which occur essentially *via* a change of the P—S bond length, appear in $550-600\,cm^{-1}$ range. The anti-phase motions $\nu P—P$ of the PS_3 groups as a whole occur *via* P—P bond length changes, give rise to the fully symmetric mode near $380\,cm^{-1}$. The deformation modes $\nu S—P—S$ due to changes in the S—P—S angles are located in the $190-260\,cm^{-1}$ region. The bending vibrations $\nu S—P—P$, *i.e.*, the bending of the PS_3 groups relative to the axis along the P—P bond, is observed as a band near $170\,cm^{-1}$. Ascribing the spectral bands in this way is conditional because a linear interaction of same symmetry internal modes in possible.

On the basis of the above information we can suppose that for $CuInP_2S_6$ crystals the internal modes of $(P_2S_6)^{4-}$ anions occur in the $140-570\,cm^{-1}$ range. The anionic librations obviously appear as bands in the $80-130\,cm^{-1}$ range. The bands in the $20-70\,cm^{-1}$ range may be attributed to translations of the Cu^+ and In^{3+} ions. The proposed identification of the low frequency bands for $CuInP_2S_6$ is confirmed by a comparison of the Raman spectra of $CdPS_3$ and $Cd_{0.87}Cu_{0.26}PS_3$, and also a comparison of the spectra for $MnPS_3$ and $Mn_{0.87}Cu_{0.26}PS_3$ and $Mn_{0.5}Ag_{1.0}PS_3$. [16]

As seen Figures 6, 7, 9, increasing the temperature and crossing the transition into the centrosymmetric paraelectric phase causes the Raman spectrum to change significantly in the range of external lattice vibrations ($10-120\,cm^{-1}$) and also that of $(P_2S_4)^{4-}$ internal modes which involve changes in the S—P—S and S—P—P angles ($140-320\,cm^{-1}$). At the transition to the paraelectric phase, the damping of the anion internal deformation modes increases drastically and the relative intensities also change (Fig. 8). The lowest energy modes in the $20-50\,cm^{-1}$ interval containing the cation translations reacts to the PT *via* an appreciable change of their frequencies (Fig. 10). Supposing that a linear interaction occurs between these modes, one may thus explain the phonon softening observed upon heating from 95 K to the vicinity of the PT. However, a resonant soft mode characteristic of a second order, displacive PT is not observed. This is

not wonder as diffraction, calorimetry and dielectric measurements all point to a first order, order–disorder PT occurring in $CuInP_2S_6$.

A abrupt rise in intensity upon warming is noticeable for the line with frequency near 33 cm^{-1} at 95 K. The intensity of the band near 28 cm^{-1} also increases. The origin of these observations may be a linear interaction of these modes with that near 42 cm^{-1}. An alternative explanation given for similar results on $Mn_{0.87}Cu_{0.26}PS_3$ crystals [16] may also be plausible. In this model the Cu atoms can occupy sites inside the layers which are constructed by $(P_2S_6)^{4-}$ anions, and also sites in the interlayer space. It is supposed that the potential wells for Cu^+ ions in the interlayer space are flatter and located higher on an energy axis. The four low frequency bands in the Raman spectrum of $CuInP_2S_6$ at 95 K may then be interpreted as follows. The line near 42 cm^{-1} is due to vibrations along the Z axis (*i.e.*, normal to the layer) of Cu^+ ions which are inside the layers, while the line near 33 cm^{-1} belongs to vibrations in the same direction of Cu^+ ions in interlayer sites. The bands near 28 and 22 cm^{-1} can be ascribed to the translational modes in which Cu^+ ions participate, and which are polarized along the X and Y-axes in the plane of the layers. In such a model, the intensity redistribution from the 42 cm^{-1} mode to that at 33 cm^{-1} testifies to the increased probability of interlayer site occupancy by Cu^+ ions as the temperature rises.

DISCUSSION OF RESULTS

The above dielectric and Raman scattering results allow one to conclude that PT order parameter fluctuations in $CuInP_2S_6$ occur in the frequency range above 10^5 Hz. Dielectric constant measurements in this frequency therefore contain full information about the crystal susceptibility anomaly in the vicinity of the phase transition. The small value of the Curie-Weiss constant confirms the order–disorder character of the PT.

At the transition from the paraelectric to the ferrielectric phase, the spontaneous polarization in $CuInP_2S_6$ appears as a consequence of the Cu^+ ions ordering within the two-well potential inside the layers and also of the In^{3+} ions shifting from centrosymmetric positions. Temperature-dependent quasielastic scattering observed in neutron spectra with a width near 5 cm^{-1} [15] most probably represent the ordering dynamics in this system. The presence of a "displacive" component in the PT order parameter fluctuation spectrum manifests in the ferrielectric phase *via* the thermal evolution of the frequencies of lattice translational modes. The eigen vectors

of this low frequency modes contain the relative translational motions of the Cu^+ and In^{3+} cations and the center of mass of the $(P_2S_6)^{4-}$ anions.

It is natural to except a linear coupling of the B_u-symmetry normal vibrations which are polarized along the Z axis perpendicular to the layers and contain the Cu^+ and In^{3+} translations in this direction, with the strongly anharmonic relaxational dynamics of the Cu^+ Cation. A significant role must also be played by the interaction of the said lattice modes with the internal vibrations of the $(P_2S_6)^{4-}$ anions having the same symmetry.

The disordering of Cu^+ cations at the transition to the paraelectric phase and their thermal "throw" into the interlayer space entail a rise in the crystal field non-uniformity within the layers as the temperature increases. This would amplify the inequivalence of the $(P_2S_6)^{4-}$ anions and causes a damping of their internal vibrations upon heating.

In relation to the above, it is important to point out that the disordering dynamics of Cu^+ ions was inferred from the Raman and infrared spectra of $CuCrP_2S_6$ *via* a breaking of the selection rules for the space group C2/c. [20]

The correlation between the temperature dependences of the damping and intensities (Fig. 8) of the anion deformation modes and that of the real part of the low frequency (10 Hz) dielectric permittivity (Fig. 2) is remarkable. For the said properties, the rate of change with temperature is largest in the 300–323 K range within the ferrielectric phase near the PT.

The "curvature" of the potential well for Cu^+ ions in the interlayer space must differ from that of the potential of such ions within the layers. Therefore, it should be possible to observe two bands in the $30-60\,cm^{-1}$ range of the Raman spectra for $CuInP_2S_6$. The same situation occurs in the case of $(Mn_{0.78}Cu_{0.26})_2P_2S_6$. [16] These bands are due to motions along the Z axis of Cu^+ ions in different potential wells. As the temperature increases, the occupancies of the named "states" for Cu^+ ions change. This fact is reflected in a redistribution of the Raman intensity of the respective spectral lines which occurs upon heating above 300 K. The rate of change is largest in the 300–323 K interval which is similar to the temperature behavior of the low frequency electric permittivity $\varepsilon'(T)$ at 10 Hz (Fig. 2).

Cu^+ ion disordering upon warming would evidently cause the spontaneous polarization to diminish. This would in turn increase the probability of the Cu^+ the thermal "throw" into the interlayer space. Such "throws" are a precondition for the appearance of ionic conductivity. The significant anharmonicity of the internal deformations of the $(P_2S_6)^{4-}$ anions which are due to changing S—P—S and S—P—P angles, gives clear spectroscopic evidence for the instability of the Cu^+ positions near the basal chalcogen planes in the investigated layered crystals.

CONCLUSIONS

In $CuInP_2S_6$ crystals, three polarization mechanisms occurring within a wide frequency range have been clearly observed and shown to be closely related to the thermal evolution of the Raman scattering. The said mechanisms and interrelating processes include: the relaxational critical slowing-down of Cu^+ hopping motions which brings about the order–disorder phase transition; the internal vibrations of the $(P_2S_6)^{4-}$ anions; the external translational lattice modes in which In^{3+} and Cu^+ ions participate; the low frequency relaxational dynamics and external $(P_2S_6)^{4-}$ deformations which "throw" the Cu^+ ions into the interlayer space; and, the ionic conductivity which follows the partial occupation of the interlayer copper sites.

The presented results point to further investigations of how non-equilibrium states due to ionic conductivity might influence the critical anomalies at the structural phase transition. It would be interesting to compare such a phenomenon with the occurrence of non-equilibrium for the electron subsystem in semiconducting $Sn_2P_2S_6$-like ferroelectrics. Also, for $MM'P_2X_6$ compounds it would be worthwhile investigating the possible existence and mechanisms for modulated (incommensurate) phases, the role of elastic deformations in dipole ordering in layered crystals, and the effect of lattice dimensionality on the critical behavior of electric dipole systems.

Acknowledgement

Part of this research is supported by the European Commission, project No ERB3512PL964434.

References

[1] Carpentier, C. D. and Nitsche, R. (1974). *Mat. Res. Bull.*, **9**, 401.
[2] Vysochanskii, Yu. M. and Slivka, V. Yu. (1992). *Sov. Phys. Usp.*, **35**, 123.
[3] Simon, A., Ravez, J., Maisonneuve, V., Payen, C. and Cajipe, V. B. (1994). *Chem. Mater.*, **6**, 1575.
[4] Barj, M., Lucazeau, G., Ouvrard, G. and Brec Eur, R. (1988). *J. Solid State Inorg. Chem.*, **25**, 449.
[5] Vysochanskii, Yu. M., Gurzan, M. I., Maior, M. M., Motria, S. F., Potorij, M. V., Salo, L. A., Khoma, M. M., Voroshilov, Yu. V. and Slivka, V. Yu. (1984). *Fiz. Tverd. Tela*, **27**, 858.
[6] Wang, Z., Willett, R. D., Laitinen, R. A. and Cleary, D. A. (1995). *Chem. Mater.*, **7**, 856.
[7] Carpentier, C. D. and Nitsche, R. (1974). *Mat. Res. Bull.*, **9**, 1097.
[8] Cajipe, V. B., Ravez, J., Maisonneuve, V., Simon, A., Payen, C., von der Muhll, R. and Fischer, J. E. (1996). *Ferroelectrics*, **185**, 135.

[9] Maisonneuve, V., Cajipe, V. B., Simon, A., von der Muhll, R. and Ravez, J. *Phys. Rev. B*, in press.
[10] Eijt, S. W. H., Currat, R. and Lorenzo e.a, J. E. (1997). *Ferroelectrics*, **202**, 121.
[11] Vysochanskii, Yu. M., Khoma, M. M. and Molnar, A. A. (1997). *Ferroelectrics*, **191**, 231.
[12] Afaf-Abdel Hady and Folk, R. (1996). *Phys. Rev. B*, **54**, 3851.
[13] Molnar, A. A., Vysochanskii, Yu. M., Horvat, A. A. and Nakonechnii, Yu. S. (1997). *Ferroelectrics*, **192**, 137.
[14] Maisonneuve, V., Reau, J. M., Dong, M., Cajipe, V. B., Payen, C. and Ravez, J. (1997). *Ferroelectrics*, **196**, 257.
[15] Cajipe, V., Payen, C., Mutka, H. and Schober, H. (1996). ILL Exper. Report, 4-02-295.
[16] Mathey, Y., Clement, R., Audiere, J. P., Poizat, O. and Sourisseau, C. (1983). *Solid State Ionics*, **9 and 10**, 459.
[17] Vysochanskii, Yu. M., Stephanovich, V. A., Molnar, A. A., Cajipe, V. B. and Bourdon, X. to be publ.
[18] Maisonneuve, V., Evain, M., Payen, C. and Cajipe, V. B. (1995). *Molinie J. of Alloys and Compounds*, **218**, 157.
[19] Vysochanskii, Yu. M., Slivka, V. Yu., Voroshilov, Yu. V., Gurzan, M. I. and Chepur, D. V. (1979). *Fiz. Tverd. Tela*, **21**, 2402.
[20] Payen, C., McMillan, P., Colombet Eur, P. (1990). *J. Solid State Inorg. Chem.*, **27**, 881.